

E. Lerche, D. Van Eester, T. Johnson, T. Hellsten, J. Ongena, M.-L. Mayoral, D. Frigione, C. Sozzi, G. Calabro, M. Lennholm, P. Beaumont, T. Blackman, D. Brennan, A. Brett, M. Cecconello, I. Coffey, A. Coyne, K. Crombe, A. Czarnecka, R. Felton, C. Giroud, M. Gatu, G. Gorini, C. Hellesen, P. Jacquet, V. Kiptily, S. Knipe, A. Krasilnikov, M. Maslov, A. Messiaen, I. Monakhov, C. Noble, M. Nocente, L. Pangioni, I. Proverbio, M. Stamp, W. Studholme, M. Tardocchi, T. Versloot, V. Vdovin, A. Whitehurst, E. Wooldridge, V. Zoita and JET EFDA Contributors

# Potential of the ICRF Heating Schemes Foreseen for ITER's Half-Field Hydrogen Phase

“This document is intended for publication in the open literature. It is made available on the understanding that it may not be further circulated and extracts or references may not be published prior to publication of the original when applicable, or without the consent of the Publications Officer, EFDA, Culham Science Centre, Abingdon, Oxon, OX14 3DB, UK.”

“Enquiries about Copyright and reproduction should be addressed to the Publications Officer, EFDA, Culham Science Centre, Abingdon, Oxon, OX14 3DB, UK.”

The contents of this preprint and all other JET EFDA Preprints and Conference Papers are available to view online free at [www.iop.org/Jet](http://www.iop.org/Jet). This site has full search facilities and e-mail alert options. The diagrams contained within the PDFs on this site are hyperlinked from the year 1996 onwards.

# Potential of the ICRF Heating Schemes Foreseen for ITER's Half-Field Hydrogen Phase

E. Lerche<sup>1</sup>, D. Van Eester<sup>1</sup>, T. Johnson<sup>2</sup>, T. Hellsten<sup>2</sup>, J. Ongena<sup>1</sup>, M.-L. Mayora<sup>13</sup>,  
D. Frigione<sup>4</sup>, C. Sozzi<sup>5</sup>, G. Calabro<sup>4</sup>, M. Lennholm<sup>3</sup>, P. Beaumont<sup>3</sup>, T. Blackman<sup>3</sup>,  
D. Brennan<sup>3</sup>, A. Brett<sup>3</sup>, M. Cecconello<sup>7</sup>, I. Coffey<sup>3</sup>, A. Coyne<sup>3</sup>, K. Crombe<sup>1</sup>,  
A. Czarnecka<sup>6</sup>, R. Felton<sup>3</sup>, C. Giroud<sup>3</sup>, M. Gatu<sup>7</sup>, G. Gorini<sup>6</sup>, C. Hellesen<sup>7</sup>,  
P. Jacquet<sup>3</sup>, V. Kiptily<sup>3</sup>, S. Knipe<sup>3</sup>, A. Krasilnikov<sup>8</sup>, M. Maslov<sup>3</sup>, A. Messiaen<sup>1</sup>,  
I. Monakhov<sup>3</sup>, C. Noble<sup>3</sup>, M. Nocente<sup>6</sup>, L. Pangioni<sup>3</sup>, I. Proverbio<sup>6</sup>, M. Stamp<sup>3</sup>,  
W. Studholme<sup>3</sup>, M. Tardocchi<sup>6</sup>, T. Versloot<sup>3</sup>, V. Vdovin<sup>9</sup>, A. Whitehurst<sup>3</sup>,  
E. Wooldridge<sup>3</sup>, V. Zoita<sup>10</sup> and JET EFDA Contributors\*

***JET-EFDA, Culham Science Centre, OX14 3DB, Abingdon, UK***

<sup>1</sup>*LPP-ERM/KMS, Association Euratom-'Belgian State', TEC Partner, Brussels, Belgium*

<sup>2</sup>*Fusion Plasma Physics, Association Euratom-VR, KTH, Stockholm, Sweden*

<sup>3</sup>*EURATOM-CCFE Fusion Association, Culham Science Centre, OX14 3DB, Abingdon, OXON, UK*

<sup>4</sup>*EURATOM-ENEA sulla Fusione, C. R. Frascati, Frascati, Italy*

<sup>5</sup>*Instituto di Fisica del Plasma, EURATOM-ENEA-CNR Association, Milan, Italy*

<sup>6</sup>*Institute of Plasma Physics and Laser Microfusion, Warsaw, Poland*

<sup>7</sup>*Uppsala University, Association EURATOM-VR, Uppsala, Sweden*

<sup>8</sup>*SRC RF Troitsk Institute for Innovating and Fusion Research, Troitsk, Russia,*

<sup>9</sup>*RNC Kurchatov Institute, Nuclear Fusion Institute, Moscow, Russia*

<sup>10</sup>*Association EURATOM-MEdC, National Institute for Plasma Physics, Bucharest, Romania*

\* See annex of F. Romanelli et al, "Overview of JET Results",

(23rd IAEA Fusion Energy Conference, Daejeon, Republic of Korea (2010)).

Preprint of Paper to be submitted for publication in Proceedings of the  
23rd IAEA Fusion Energy Conference, Daejeon, Republic of Korea  
(10th October 2010 - 16th October 2010)



## ABSTRACT.

To extend the knowledge on the performance of the Ion Cyclotron Resonance Frequency (ICRF) heating schemes in the non-activated half- $B_0$  phase of ITER, a detailed assessment of the fundamental H and the 2<sup>nd</sup> harmonic  $^3\text{He}$  ICRF heating scenarios in majority H plasmas was undertaken. The numerical studies were performed using the 1D TOMCAT [1] and the 2D CYRANO [2] codes adopting the equilibrium profiles computed for the initial operation phase of ITER [3]. To have an experimental backing of the computations, the nominal ITER half-field of 2.65T and the ICRF frequencies for those heating scenarios ( $f=42\text{MHz}$  for fundamental H and  $f=53\text{MHz}$  for 2<sup>nd</sup> harmonic  $^3\text{He}$  heating) were closely reproduced in dedicated experiments performed in the JET tokamak [4].

## 1. INTRODUCTION

The non-active phase of ITER will start with Hydrogen plasmas at reduced magnetic field. At the nominal half-field of  $B_0 = 2.65\text{T}$  and with the auxiliary power currently foreseen to be available in this phase, 16.5MW off-axis Neutral Beam Injection (NBI), 15MW off-axis electron-cyclotron heating (ECE) and 10MW on-axis ion cyclotron resonance (ICRF) heating, the discharges are expected to be in L-mode and typical central densities of  $n_0 \approx 3 \times 10^{19}/\text{m}^3$  and central temperatures of approximately  $T_i = 8\text{keV}$  and  $T_e = 10\text{keV}$  were estimated [3]. In these calculations, it was envisaged that 10MW of ICRF power would be sufficient for raising the ion and electron temperatures from  $T_i \approx T_e = 5\text{keV}$  to  $T_i = 8\text{keV}$  and  $T_e = 10\text{keV}$ , respectively, if central ICRF heating with equal power sharing between electrons and ions is considered. This seems a rather optimistic statement and assumes that all the power launched by the ICRF antenna is absorbed in the core of the plasma. Unlike for  $^4\text{He}$  (or D) plasmas, for which standard H minority ICRF heating could be used, in H plasmas and for the designed frequency range of the ICRF heating system in ITER ( $f = 40\text{-}55\text{MHz}$ ), only fundamental ion cyclotron heating of H majority ions at  $f \approx 42\text{MHz}$  (referred here as  $N = 1$  H heating) and 2<sup>nd</sup> harmonic ion cyclotron heating of  $^3\text{He}$  ions at  $f \approx 53\text{MHz}$  (referred here as  $N = 2$   $^3\text{He}$  heating) are feasible scenarios for central ion heating at the nominal half-field of  $B_0 = 2.65\text{T}$ . However, both are characterized by poor ion absorption: The  $N = 1$  H majority scenario suffers from the adverse polarization of the RF fields close to the ion cyclotron resonance layer of the majority H ions ('screening effect') whereas the  $N = 2$   $^3\text{He}$  heating scheme requires a relatively large fraction of 'minority' ions to become efficient. Results of recent JET experiments [4] and preliminary numerical simulations of the ICRF heating scenarios for ITER's half-field phase in H plasmas indicate that relatively low single-pass RF power absorption with dominant fastwave electron heating will take place, and that high heating efficiencies (as those typically observed in fundamental ICRF minority heating) will be unlikely. Given the fact that ITER will rely heavily on every MW of auxiliary heating power that can be injected into the plasma, numerical and experimental investigations aiming at testing and optimizing the ICRF heating performance of these scenarios are very important for a successful operation of ITER in its early Hydrogen phase.

## 2. SUMMARY OF JET EXPERIMENTS

The ICRF parameters of the half-field phase of ITER were closely reproduced in recent JET experiments [4]: The  $N = 1$  H heating scenario was studied at  $f = 42.5\text{MHz}/B_0 = 2.65\text{T}$  and the  $N = 2$   $^3\text{He}$  heating experiments were done at  $f = 51.5\text{MHz}/B_0 = 2.65\text{T}$ . In these conditions, the fundamental ion cyclotron resonance layer of the H ions and the 2nd harmonic ion cyclotron resonance of the  $^3\text{He}$  ions are both located near the plasma centre. The antenna phasing was dipole in both cases and up to 5.5MW of ICRF power was coupled to the plasma. Aside from the different ICRF parameters and the dilution of the H plasmas with  $^3\text{He}$  in the  $N = 2$   $^3\text{He}$  heating pulses (no  $^3\text{He}$  was injected in the  $N = 1$  H heating pulses), the plasmas were similar in the two sessions. Both experiments were performed in L-mode and adopted a plasma geometry that favours the ICRF antenna coupling, with antenna strap - plasma separatrix distances around 9.5-11.0cm. Typical central densities of  $n_0 = 3 \times 10^{19}/\text{m}^3$  and central temperatures ranging from  $T_e = 2\text{-}4\text{keV}$ , depending on the NBI power applied ( $0 < P_{\text{NBI}} < 8\text{MW}$ ), were obtained in the discharges. Although the central densities of the JET experiments are comparable to those expected in the initial phase of ITER, both electron and ion temperatures are well below leading to a different collisional regime than the one expected in ITER.

The experimental ICRF heating efficiencies ( $\eta = \text{power transferred to the plasma/coupled power}$ ) for electrons and (bulk) ions obtained by analyzing, respectively, the ECE and charge-exchange signal responses to fast variations in the applied ICRF power [5] are depicted in Fig.1 for the fundamental H majority experiments (left) and for the 2nd harmonic  $^3\text{He}$  heating experiments (right). The prompt response of the electron temperature to the ICRF power variations confirm that in both scenarios the electron absorption is mainly due to direct fast wave Landau damping (ELD) and Transit Time Magnetic Pumping (TTMP) and not to collisional slowing-down of ICRF accelerated ions, as is usually the case in minority ICRF heating schemes. For the H majority case, the electrons absorb typically twice as much RF power as the ions and both absorptivities increase with the central plasma temperature, reaching a total heating efficiency of  $\eta \approx 0.4$  at  $T_{e0} = 2.5\text{keV}$ . The slope of the heating efficiency of the ions is somewhat steeper than the one for the electrons, indicating that the ion cyclotron absorption of the H ions is more privileged than the electron absorption when increasing the bulk plasma temperature within the studied range. For the  $N = 2$   $^3\text{He}$  scenario, the dependence of the heating efficiency with the temperature was minor, but a clear enhancement of the ICRF absorption for higher  $^3\text{He}$  concentrations was observed. Note that it is the ion heating that is mainly improved at higher  $^3\text{He}$  concentrations and that the total heating efficiency reached at  $X[^3\text{He}] \geq 20\%$ , where the ion absorption exceeds that of the electrons, is similar to the one obtained for the H majority case ( $\eta \approx 0.3\text{-}0.4$ ). The ion absorption at low  $X[^3\text{He}]$  (as currently proposed for ITER) is very small and the total heating efficiency is only about  $\eta \approx 0.2$  in these conditions.

As mentioned, the experimental RF heating efficiencies obtained in both scenarios (compared to typical heating efficiencies of  $\eta \geq 0.8$  observed in minority ICRF heating schemes) were anticipated to be low: Fundamental majority ICRF heating suffers from the near-vanishing values of the left-hand polarized RF electric field component close to the ion cyclotron resonance layer whilst second

harmonic heating scenarios typically require large fractions of the minority species to be efficient. Despite the low efficiencies of these heating schemes, fast H ions up to 50keV and fast  $^3\text{He}$  ions up to 200keV were detected by the Neutral Particle Analyser (NPA) diagnostics in the  $N = 1$  H and in the  $N = 2$   $^3\text{He}$  heating experiments, respectively, when 5MW of RF power was applied.

An important consequence of the low ICRF absorptivity of these heating scenarios is the enhancement of plasma-wall interactions leading to relatively large impurity content and considerable radiation losses in the plasma. This is depicted in Fig.2 (left), where the total radiated power is shown as function of the ICRF power applied for the  $N = 1$  H (circles) and the  $N = 2$   $^3\text{He}$  (triangles) heating experiments. The data correspond to 0.4s time averaged values sampled throughout the pulses. The density, temperature and NBI power ( $\sim 1.3\text{MW}$ ) were similar in all the time intervals considered.

The fact that the radiation losses for a given ICRF power level are higher for the  $N = 2$   $^3\text{He}$  case than for the fundamental H majority case is not only due to the presence of relatively large fractions of  $^3\text{He}$  in the plasma (higher  $Z_{\text{eff}}$ ), but is also related to a stronger RF-induced plasma-wall interaction observed in this case, leading to a higher impurity content in the plasma. This is depicted in Fig.2 (right), where the line emission intensity of Beryllium measured by visible spectroscopy is shown as function of the ICRF power for the two scenarios. The same time intervals as on the left figure were considered. A similar study for the  $\text{C}^{+6}$  and  $\text{C}^{+4}$  spectroscopy measurements (not shown) supported by 2D bolometer tomography indicates that most of the additional radiation observed in the  $N = 2$   $^3\text{He}$  case comes from the plasma edge rather than from the bulk plasma. The fact that the impurity content is higher for this case than for the fundamental H majority case despite the similar ICRF heating efficiencies (and similar antenna coupling conditions) is believed not only to be related to the different RF sheath rectification effects at the two distinct operation frequencies but also to the different fast ion losses observed in the two cases. As a matter of fact, when more than 5MW of NBI was applied together with the ICRF power in the  $N = 2$   $^3\text{He}$  discharges, ICRF accelerated D-beam ions in the MeV range (detected with  $\gamma$ -spectroscopy) were observed [6] These ions accelerated to high energies lead to enhanced number of fast ion losses when compared to the fundamental H majority heating case (where the parasitic D absorption was practically negligible).

### 3. PRELIMINARY NUMERICAL SIMULATIONS FOR ITER

The numerical simulations of the fundamental H majority and the  $N = 2$   $^3\text{He}$  heating schemes proposed for ITER's initial Hydrogen phase were performed at  $B_0 = 2.65\text{T}$  ( $I_p = 7.5\text{MA}$ ) with  $f = 42\text{MHz}$  and  $f = 53\text{MHz}$ , respectively. The equilibrium profiles computed for 41.5MW of NBI + ECRH + ICRF auxiliary power ( $n_0 = 3.33 \times 10^{19}/\text{m}^3$ ,  $T_i = 8\text{keV}$ ,  $T_e = 10\text{keV}$ ) were adopted in the calculations and parametric scans on plasma density, temperature,  $^3\text{He}$  concentration and antenna phasing were done to assess their impact on the ICRF absorptivity.

In figure 3, the power absorption profiles obtained for the fundamental H (left) and for the  $N = 2$   $^3\text{He}$  (right) heating schemes with the 1D TOMCAT code [1] using the plasma parameters mentioned

above are depicted. The dominant toroidal mode ( $n_\phi = 34$ ) of the ITER antenna spectrum in  $0\pi\pi 0$  phasing was adopted and 4% of  $^3\text{He}$  (with a density profile similar to the one used for the H majority) was considered in the  $N = 2$   $^3\text{He}$  heating simulations.

It is clear that in both cases direct fast-wave electron heating is the dominant absorption process and that the minority species in the  $N = 2$   $^3\text{He}$  heating scheme only absorbs a very small amount of the total power at these low concentrations (by increasing  $X[^3\text{He}]$  the ion absorption is gradually enhanced as will be shown later). Also note that parasitic absorption of H ions is possible at the high-field side in this scenario, particularly if high energy Hbeams would be used. In the conditions depicted in Fig.3, the relative single-pass absorption of the ICRF power ( $\mu = \text{power absorbed in a single-pass through the plasma} / \text{power launched at the low-field side boundary}$ ) is only about  $\mu = 0.3$  for the  $N = 1$  H heating scheme and about  $\mu = 0.25$  for the  $N = 2$   $^3\text{He}$  scenario. Possible means of enhancing these low absorptivities by changing some of the plasma parameters will be presented next.

In figure 4 the single-pass absorptions of the individual plasma species in the  $N = 1$  H majority heating scenario obtained as function of the H temperature (left) and of the plasma central density (right) are illustrated. By increasing the H temperature, the ion absorption is strongly enhanced due to the Doppler-shift broadening of the H cyclotron resonance layer. At  $T_H \approx 20\text{keV}$ , the ion absorption becomes dominant (the electron temperature was kept constant at  $T_e = 8\text{keV}$  in these simulations). The increase in the plasma central density leads to a strong enhancement of the total single-pass absorption, mainly due to more efficient (fast wave) electron heating. Nevertheless, if operating at high densities, the collisional energy equipartition between electrons and ions is also more efficient and the fact that most of the ICRF power goes into the electron channel rather than directly into the ion channel may be of secondary importance.

In figure 5 the variation of the single-pass absorptions of the plasma species in the  $N = 2$   $^3\text{He}$  heating scheme as function of the  $^3\text{He}$  concentration (left) and as function of the plasma central density (right) is illustrated. As expected by simple theory (and as suggested in the JET experiments), the  $^3\text{He}$  absorption is gradually increased when the fraction of  $^3\text{He}$  ions is larger in the plasma while the electron absorption is virtually insensitive to the  $^3\text{He}$  concentration. However, for the ITER conditions (where the fast-wave electron absorption at the LFS always plays a considerable role in the ICRF power balance), the  $^3\text{He}$  power absorption is practically negligible at low concentrations and one would need as much as  $X[^3\text{He}] \approx 30\%$  in the plasma to achieve dominant ion heating. The dependence of the ICRF power absorption with the plasma density is similar to the one obtained for the  $N = 1$  H heating case, showing a strong increase when the central density is augmented but mainly due to enhanced electron heating (the absorption by the  $\text{He}^3$  ions being practically negligible in these conditions). For the  $N = 2$   $^3\text{He}$  scenario, the dependence of the ICRF absorption with the  $^3\text{He}$  temperature is weak: effective temperatures of approx.  $150\text{keV}$  are needed to achieve dominant ion heating at  $X[^3\text{He}] = 4\%$ . It is important to mention that in both cases, the formation of RF-induced ion tails may have an impact on the heating performances and on the ICRF power distribution amongst the various species. This non-linear effect requires coupled wave / Fokker-Planck simulations and



has not been considered in the present study (see e.g. [7] for an example of such calculations).

The influence of the antenna spectrum on the ICRF power absorption for the  $N = 1$  H majority (left) and of the  $N = 2$   $^3\text{He}$  (centre and right) heating schemes is depicted in Fig.6. For the latter, the centre and right figures correspond to  $X[^3\text{He}] = 4\%$  and  $X[^3\text{He}] = 30\%$  respectively. The considered plasma density and temperatures were  $n_0 = 3.3 \times 10^{19}/\text{m}^3$  and  $T_i = 8\text{keV} / T_e = 10\text{keV}$  in all three cases. The various points corresponding to different antenna phasings (indicated in the left figure) were obtained by convoluting the relative power absorptions obtained in individual toroidal mode number simulations with the various antenna spectra calculated by the ANTITER II code [8] for the ICRF antenna being designed for ITER. The abscissae represent the dominant parallel wavenumber  $k_{//} = n_{\phi}/R$  (where  $n_{\phi}$  is the toroidal mode number and  $R$  is the antenna major radius) of the antenna spectra launched for each given phasing configuration.

For the  $N = 1$  H majority heating scheme, it is clear that operating at antenna phasings with higher  $k_{//}$  values (e.g. dipole) privileges the overall ICRF power absorption, but the power sharing between ions and electrons is roughly similar in the various phasings. For the low concentration  $^3\text{He}$  heating scheme, the power absorption also strongly increases with  $k_{//}$  but the scenario is completely dominated by electron absorption independent of the antenna phasing. The most interesting case is perhaps the high concentration  $N = 2$   $^3\text{He}$  scenario (right), for which the total absorption is not as sensitive to  $k_{//}$  but the power sharing between ions and electrons is strongly influenced by the antenna phasing: At low  $k_{//}$  ion heating is clearly dominant whilst at high  $k_{//}$  electron absorption becomes more important. At intermediate  $k_{//}$  both species absorb approximately the same fraction of the ICRF power injected. Therefore, for the  $^3\text{He}$  heating scenario with large minorities, operating at  $00\pi\pi$  (or  $0\pi\pi0$ ) phasing would be preferred to operating in dipole ( $0\pi0\pi$ ) to achieve satisfactory bulk ion heating.

From the simulations presented it is clear that the two heating scenarios available for the half-field ITER operation in Hydrogen have marginal efficiencies, in particular because the plasma density and the plasma temperature in the early operation phase are relatively modest. Moreover, because of ITER's large volume (and the high price of  $^3\text{He}$ ), the  $^3\text{He}$  concentrations considered for its operation should be kept to relatively small level ( $<5\%$ ). This limited operational domain obviously restricts the means for optimizing the ICRF heating schemes and further investigation and/or search for alternative scenarios are essential for a successful performance of the ITER H plasmas. One possibility that was not mentioned so far is the effect of the plasma dilution (with another ion species) on the heating efficiency of the  $N = 1$  H heating scheme via modifications of the RF field polarization near the cyclotron resonance layer. Preliminary simulations suggest that this effect is relatively weak for low concentrations of the second ion species but the experimental results of the  $N = 1$  H majority heating scenario in JET have shown indications of a considerable increase in the ICRF heating efficiency when  $\sim 4\%$  of  $^4\text{He}$  is present in the H plasmas with respect to pure H discharges. Another interesting alternative for efficient ICRF heating of the ITER H plasmas would be to operate at  $1/3$  of the nominal magnetic field ( $B_0 = 1.8\text{T}$ ), where second harmonic H

heating can be used. Preliminary simulations show that this heating scheme is characterized by full single-pass absorption ( $\mu = 1$ ) with dominant bulk ion heating, as depicted in Fig.7, where the power absorption profiles of the  $N = 2$  H heating scheme computed by the TOMCAT code with the half-field equilibrium parameters for ITER are illustrated (left). Note the strong decrease of the E+ component of the RF electric field (right) near the ion cyclotron resonance layer indicating the efficient absorption of the ICRF power in this region. If the confinement properties of the H plasmas at 1.8T are not much degraded with respect to the ones at 2.65T, then this scenario could be a potential alternative for efficient plasma heating and for efficient commissioning of the ICRF system in the early operation phase of ITER.

## SUMMARY

The ICRF heating schemes proposed for ITER's half-field H phase were examined. Unlike the standard H minority ICRF heating scenario foreseen for the operation in  $^4\text{He}$  plasmas [9] (which has high single-pass absorptivity and thus is expected to yield good heating performance), it was found - both via simulations and experimentally in JET - that the heating schemes available for the H plasma operation have a poor heating efficiency for the typical plasma parameters expected in the initial ITER phase. The simulations have shown that fast-wave electron heating will dominate in both the fundamental H majority and in the 2<sup>nd</sup> harmonic  $^3\text{He}$  ICRF heating schemes, particularly at the rather modest densities and temperatures expected in ITER's initial operation phase. The power absorptivity of both scenarios is small, because of the adverse polarization of the RF fields in the fundamental H majority ICRF heating case and because of the low minority concentrations expected in the ITER plasmas for the  $N = 2$   $^3\text{He}$  heating case. Increased plasma density and temperature both help to enhance the ICRF power absorption but in general electron rather than ion damping is primarily improved. For the fundamental H majority heating case, the ion temperature plays a major role on the scenario's performance but ion temperatures of about 20keV are necessary to achieve dominant ion heating (with a total single-pass absorption of  $\mu \approx 0.4$ ). For the  $N = 2$   $^3\text{He}$  ICRF heating case, the ion temperature has a weaker influence and the  $^3\text{He}$  concentration is the main actuator on the heating performance. However, the simulations suggest that high concentrations ( $X[^3\text{He}] \approx 30\%$ ) are needed to achieve prevailing ion heating, with a total single-pass absorption of  $\mu \approx 0.45$ . The absorptivity is only about  $\mu \approx 0.25$  for the typical  $X[^3\text{He}] = 4\%$  value originally proposed for ITER. Whilst for the  $N = 1$  H majority heating case and for the  $N = 2$   $^3\text{He}$  heating scheme with low  $X[^3\text{He}]$  operating at high  $k_{\parallel}$  antenna phasing (e.g. dipole) leads to larger RF absorptivities, low  $k_{\parallel}$  phasing (e.g.  $0\pi\pi 0$ ) would be preferred in the  $N = 2$   $^3\text{He}$  heating scenario with large  $X[^3\text{He}]$  for privileging ion heating. Given the relatively poor performance of the ICRF heating scenarios in the ITER half-field Hydrogen phase, it is important to search for means of enhancing their efficiency. One possibility that is being investigated (and for which there were indications in the experiments performed in JET) is the dilution of the H plasmas with a second ion species (e.g.  $^4\text{He}$ ), which - via a change in the RF field structure in the plasma - could crank up the

heating efficiency of the fundamental H majority heating scenario. Alternatively, by operating at a further reduced magnetic field (1/3 of the nominal field), second harmonic heating of the H majority plasmas at  $f \approx 53\text{MHz}$  becomes accessible. Numerical simulations indicate that this heating scenario features high single-pass absorption with dominant ion heating and thus could lead to large heating efficiencies if the confinement properties of the H plasmas at this reduced field are not too poor. Experimental investigations of this scenario as well as further optimization of the  $N = 1$  H majority and the  $N = 2$   $^3\text{He}$  ICRF heating schemes are planned in future.

## ACKNOWLEDGEMENTS

The authors would like to thank Dr. P. Lamalle for the discussions on the initial ICRF scenarios foreseen for ITER. This work was supported by EURATOM and carried out within the framework of the European Fusion Development Agreement. The views and opinions expressed herein do not necessarily reflect those of the European Commission.

## REFERENCES

- [1]. D. Van Eester et al., Plasma Physics and Controlled Fusion **40** (1998) 1949–1975
- [2]. P.U. Lamalle (1994) PhD Thesis LPP-ERM/KMS Report **101**, Université de Mons
- [3]. A. Loarte and P. Lamalle, private communications
- [4]. E.A. Lerche et al., O4.121, 37th EPS Conf. on Controlled Fusion and Plasma Physics, Dublin (2010)
- [5]. E.A. Lerche et al., Plasma Physics and Controlled Fusion **50** (2008) 035003
- [6]. V. Kiptily et al., to appear in special TF-H issue of Plasma Physics and Controlled Fusion
- [7]. L.-G. Eriksson, T. Hellsten and U. Willén, Nuclear Fusion **33** (1993) 1037
- [8]. A. Messiaen et al., Nuclear Fusion **50** (2010) 025026
- [9]. R. Budny et al., paper OV/1-3, this conference

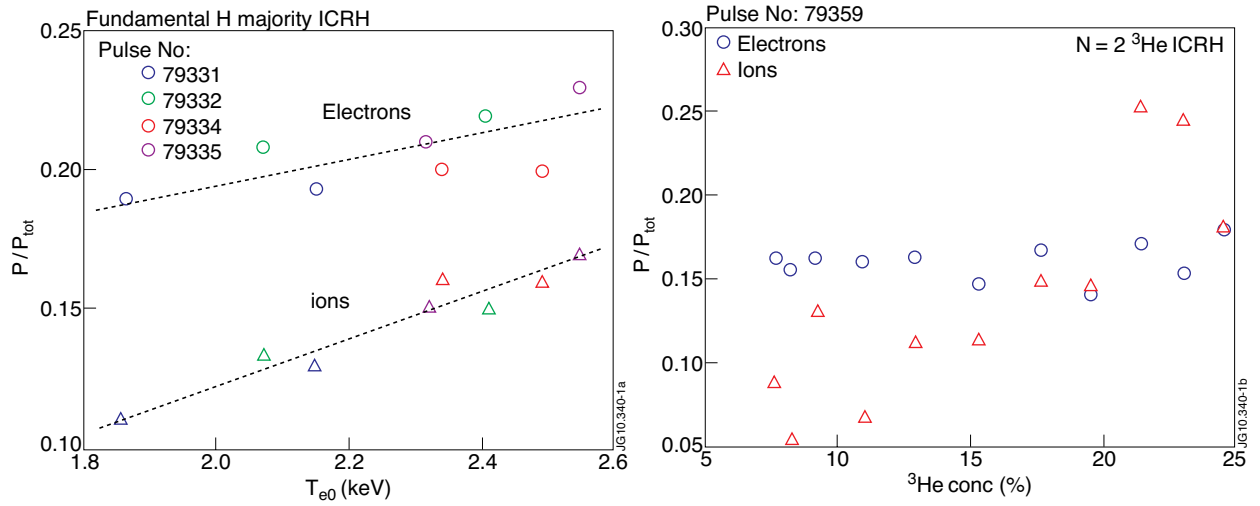


Figure 1: (Left) Ion (triangles) and electron (circles) heating efficiencies as function of the central plasma temperature for a series of discharges of the fundamental H majority ICRF scenario in JET; (Right) Ion (triangles) and electron (circles) heating efficiencies as function of the  $^3\text{He}$  concentration for a discharge of the  $N = 2$   $^3\text{He}$  ICRF scheme, in which a ramp-up of the  $^3\text{He}$  concentration from 8- 25% was imposed.

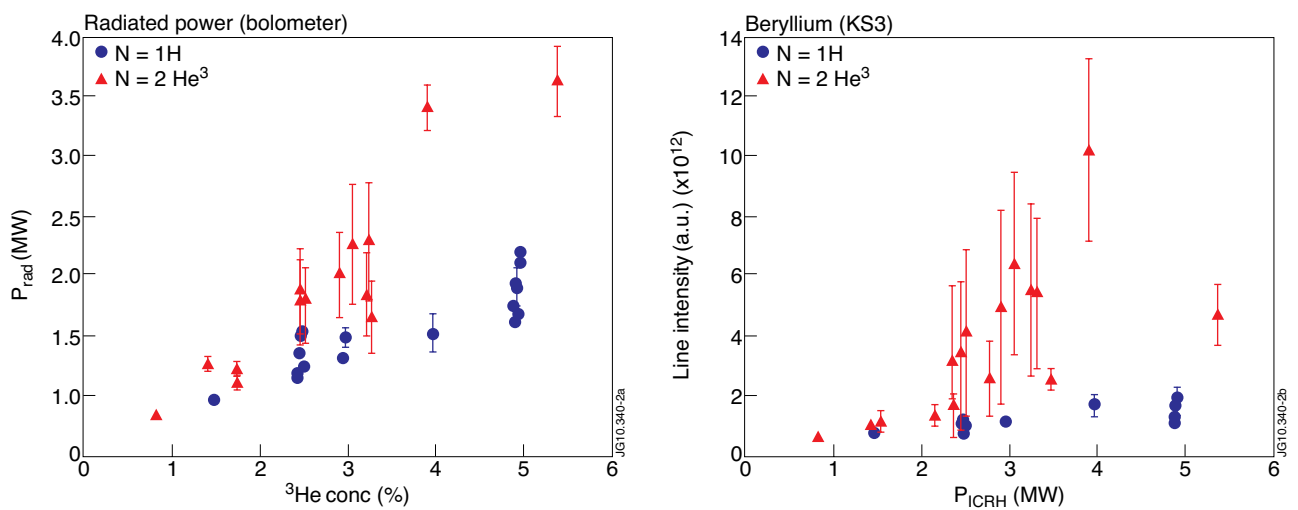


Figure 2: Total radiated power (left) and intensity of Be line (right) as function of the ICRF power for the  $N = 1\text{H}$  (circles) and the  $N = 2$   $^3\text{He}$  (triangles) ICRF heating schemes. The data correspond to 0.4s time averaged values throughout the discharges with similar densities, temperatures and NBI power.

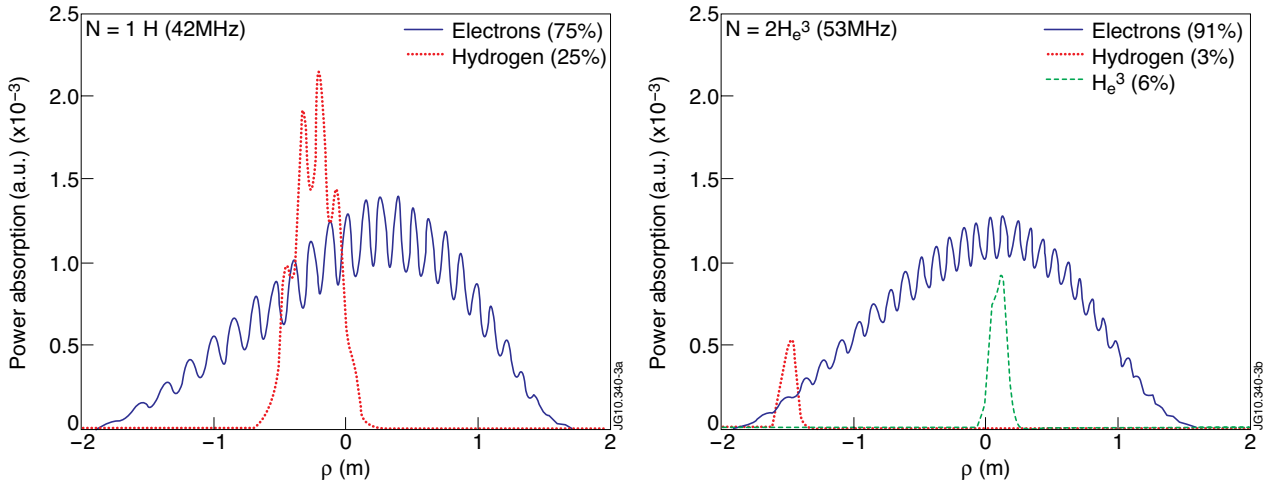


Figure 3: Power absorption profiles computed for the  $N=1$  H (left) and for the  $N = 2$   $^3\text{He}$  (right) heating scenarios for the initial ITER H plasmas at  $B_0=2.65\text{T}$ . For the latter 4%  $^3\text{He}$  was considered in the plasma. The absorbed power fractions are indicated in the legends.

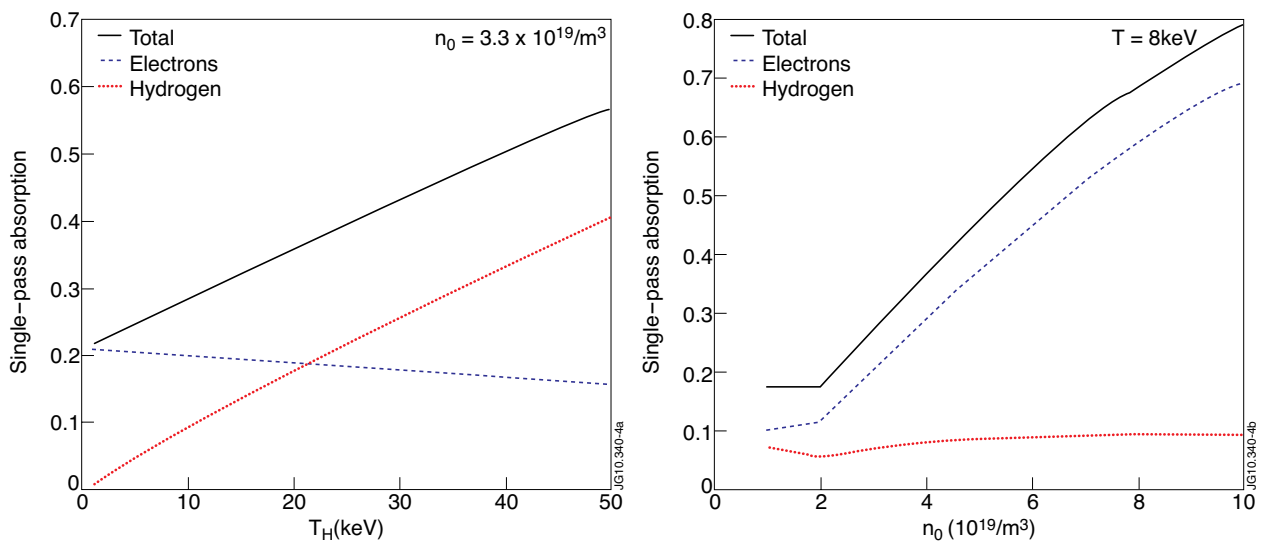


Figure 4: Dependence of the single-pass absorptivities of the plasma species as function of the Hydrogen temperature (left) and the plasma density (right) for the fundamental H majority heating scenario in ITER's half-field phase.

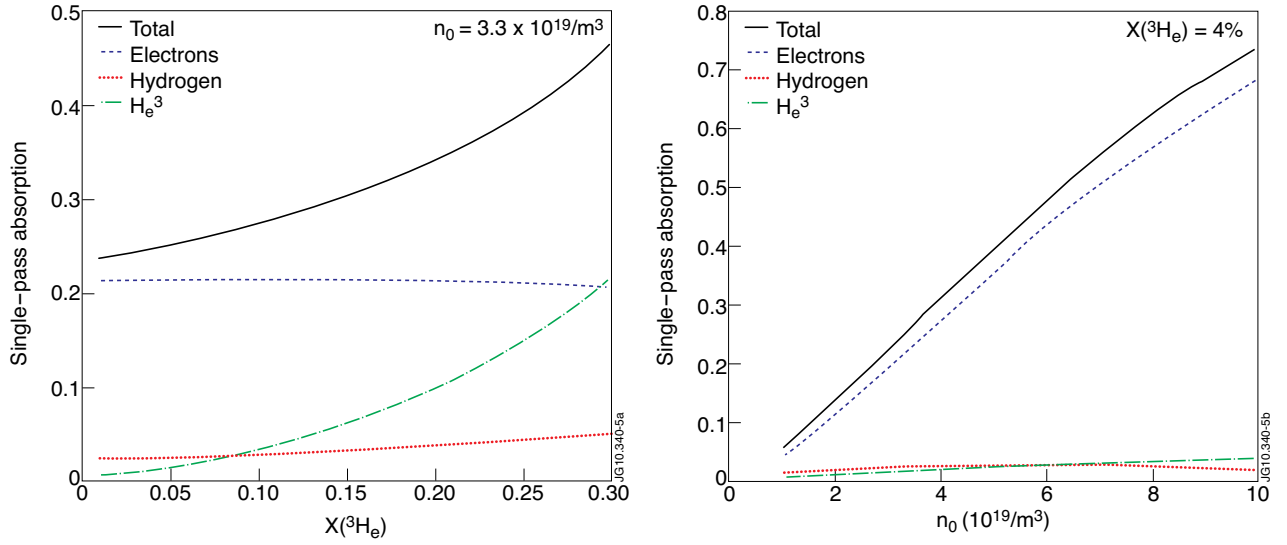


Figure 5: Dependence of the single-pass absorptivities as function of the  $^3\text{He}$  concentration (left) and of the plasma density (right) for the fundamental  $N = 2$   $^3\text{He}$  heating scenario in ITER's half-field phase.

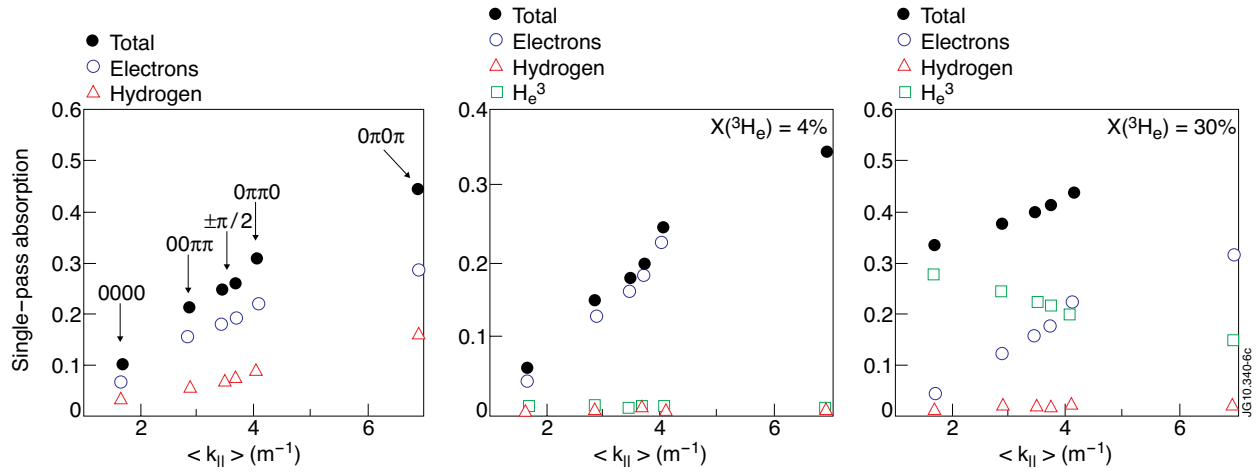


Figure 6: Influence of the antenna phasing on the ICRF power absorptivities: (left)  $N=1$  H majority heating scheme; (centre)  $N = 2$   $^3\text{He}$  heating scheme with  $X[^3\text{He}] = 4\%$ ; (right)  $N = 2$   $^3\text{He}$  heating scheme with  $X[^3\text{He}] = 30\%$ .

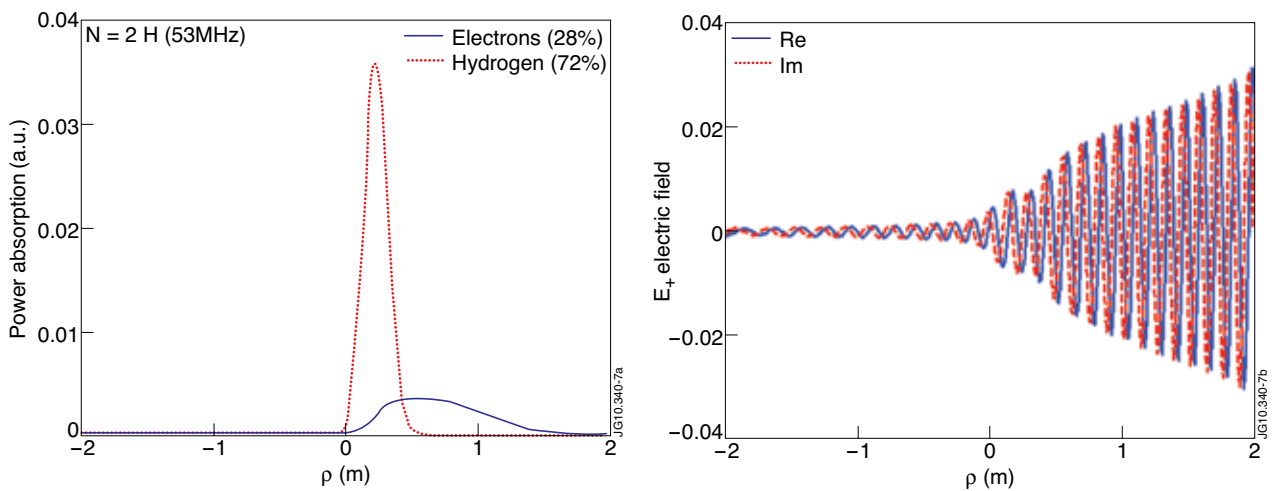


Figure 7: (left) Power absorption profiles for the  $N = 2$  H majority ICRF heating scenario in ITER at  $B_0 = 1.8\text{T}$  and  $f = 53\text{MHz}$ ; (right) Corresponding left-hand polarized ( $E_+$ ) RF electric field component.